THE ASTROPHYSICAL JOURNAL, 324:379–390, 1988 January 1

QUASI-PERIODIC OSCILLATIONS IN THE X-RAY FLUX OF THE RAPID BURSTER (MXB 1730−335)

L. STELLA,[1,2] F. HABERL,[1] W. H. G. LEWIN,[3] A. N. PARMAR,[1] J. VAN PARADIJS,[4] AND N. E. WHITE[1]

Received 1987 March 23; accepted 1987 June 17

ABSTRACT

We report on the results of an *EXOSAT* observation of the "Rapid Burster" in 1985 August during an active state. Forty 1–10 minute long type 2 bursts were detected together with persistent emission. Quasi-periodic oscillations (QPO) were observed in 23 bursts with frequencies between 2 and 5 Hz. The average frequency of the QPO during the bursts was anticorrelated with the average burst flux, and the rms strength of the QPO was as high as ∼20% during the longest bursts. QPO from the Rapid Burster were first reported by Tawara *et al.* who found ∼2 Hz oscillations during two out of 63 type 2 bursts. During the *EXOSAT* observation QPO with rms strength up to ∼35% were also observed occasionally in the persistent emission after relatively short (1–2 minutes) bursts. In several cases the QPO frequency evolved from ∼4 Hz after a burst to ∼2 Hz in 3–6 minutes, without a general correlation with the flux of the persistent emission. Variations in QPO frequency measured in the persistent emission were positively correlated with the spectral hardness, such that the spectrum softened as the QPO frequency decreased. QPO with frequencies ranging between 0.4 and 1 Hz were also observed occasionally during intervals of 1–3 minutes before bursts. On one occasion two QPO frequencies were observed simultaneously, at 0.44 and 0.88 Hz, consistent with a frequency ratio of 2.

Comparatively weak red noise (RN) was usually detected shortward of ∼1 Hz with an rms strength of less than 6% (0.06–1 Hz range). In most cases the RN strength was far smaller than the corresponding QPO strength (up to a factor of ∼14 for the longest burst observed).

Among the models for QPO in low-mass X-ray binaries (LMXRB) that involve the presence of a neutron star magnetosphere, only the beat frequency model is still consistent with the QPO properties of the Rapid Burster, but only in a very qualitative way. Nonmagnetospheric models for QPO involving neutron star oscillations, scattering in an accretion disk corona, or magnetic activity in the boundary layer between an accretion disk and a weakly magnetized neutron star are ruled out. Obscuration of the central X-ray source by an oscillating accretion disk rim also provides a viable scenario for the generation of the QPO from the Rapid Burster.

Subject headings: stars: pulsations — X-rays: binaries — X-ray: bursts

I. INTRODUCTION

It has been clear since its discovery in 1976 (Lewin *et al.* 1976) that the Rapid Burster MXB 1730−335 displays unique X-ray burst properties. It produces two very different kinds of X-ray bursts (Hoffman, Marshall, and Lewin 1978). Type 1 bursts, which are similar to those observed from ∼35 other burst sources, show a distinct spectral softening as they decay; these are most probably due to thermonuclear flashes on the surface of an accreting neutron star (Woosley and Taam 1976; Maraschi and Cavaliere 1977; Joss 1978; for a review see Lewin and Joss 1983). The bursts classified as type 2 do not exhibit such a pronounced spectral evolution, and they generally show a considerable range in duration (from a few seconds to ∼11 minutes) and recurrence interval (from ∼10 s to ∼1 hr). Their recurrence behavior is similar to that of a relaxation oscillator, with the integrated flux in each burst roughly proportional to the time interval to the next burst (Lewin *et al.* 1976; Mason, Bell-Burnell, and White 1976; Ulmer *et al.* 1977; White *et al.* 1978; Marshall *et al.* 1979; Inoue *et al.* 1980; Basinska *et al.* 1980; Kunieda *et al.* 1984*a*). The type 2 bursts display a great variety in their shape and are unique to the Rapid Burster (Lewin and Joss 1983, and references therein).

The long-term activity of the Rapid Burster has a recurrent transient character with intervals of ∼6 months; the active periods typically last for a few weeks (Lewin 1977*b*; Grindlay and Gursky 1977; see Lewin and Joss 1983 for a review). During its active intervals it displays various combinations of bursting modes and strength of persistent emission. There are times when only type 2 bursts are observed with high- or low-level persistent emission between them (Lewin *et al.* 1976; Mason, Bell-Burnell, and White 1976; Marshall *et al.* 1979; van Paradijs, Cominsky, and Lewin 1979; Inoue *et al.* 1980; Basinska *et al.* 1980). At other times both type 1 and type 2 bursts are observed (Hoffman, Marshall, and Lewin 1978; Marshall *et al.* 1979). There are also periods when strong persistent emission and only type 1 bursts are detected (Kunieda *et al.* 1984*b*; Barr *et al.* 1987).

A great deal of interest has been recently raised in connection with the discovery of fast (1–50 Hz) quasi-periodic oscillations (QPO) in the X-ray flux of nine bright galactic bulge and globular cluster X-ray sources (GX 5-1, van der Klis *et al.* 1985; Sco X-1, Middleditch and Priedhorsky 1986; Cyg X-2, Hasinger *et al.* 1986; GX 17+2, Stella, Parmar, and White 1985, 1987; Langmeier *et al.* 1985; GX 349+2, Lewin *et al.*

[1] *EXOSAT Observatory*, Astrophysics Division, Space Science Department, European Space Agency, ESTEC, The Netherlands.
[2] On leave from I.C.R.A., Department of Physics "G. Marconi," University of Rome, Italy.
[3] Massachusetts Institute of Technology, Center for Space Research and Physics Department, Cambridge, MA 02139.
[4] Astronomical Institute "Anton Pannekoek," University of Amsterdam, The Netherlands.

1986; Cooke, Stella, and Ponman 1985; 4U 1820−30, Stella, White, and Priedhorsky 1985, 1987; GX 3+1, Lewin *et al.* 1987; Cir X-1, Tennant 1987; GX 340+0, van Paradijs *et al.* 1987; see also Norris and Wood 1985; Elsner *et al.* 1986).

During *Hakucho* observations in 1979, when the Rapid Burster was producing type 2 bursts which varied in duration from ~0.7 to ~10 minutes, ~2 Hz pulsations were detected in two out of 63 bursts (Tawara *et al.* 1982). Since the pulsation period measured from the two bursts differed by ~1%, Tawara *et al.* (1982) ruled out that the pulsations resulted directly from the rotation of a neutron star.

We report here on an *EXOSAT* observation of the Rapid Burster made on 1985 August 28–29. The Rapid Burster was active, showing many "flat-topped" type 2 bursts and persistent emission between bursts. We find a unique variety of QPO behavior during bursts, with frequencies ranging between 2 and 5 Hz. In addition, QPO were sometimes found in the persistent emission between bursts, with average frequencies between 0.4 and 4.5 Hz. A few preliminary results have already been reported by us (Stella *et al.* 1985; Stella 1986; Lewin 1986*a*). The details of the observation together with the light curves are given in § II, and the properties of the QPO are presented in § III. The energy spectra of the bursts and persistent emission are described in § IV. In § V we discuss these results in relation to the QPO seen from other X-ray binaries and compare them with current QPO models. A summary of the possible model confrontations is presented in § VI.

II. OBSERVATIONS

The Rapid Burster lies only 25′ from another burst source, 4U/MXB 1728−34, and a pointed *EXOSAT* observation directly at one leaves the other in the 45′ full width half-maximum (FWHM) field of view (FOV) of the medium energy (ME) instrument (see Barr *et al.* 1987). An *EXOSAT* observation of MXB 1728−34 that began on 1985 August 28 at 15:30 UT revealed long "flat-topped" bursts, characteristic of the type 2 bursts seen from the Rapid Burster. For the first 2.3 hr the Rapid Burster was at a collimator transmission efficiency of 41%. For a 15 minute interval around 16:30 UT, when the satellite was still pointing at MXB 1728−34, half of the ME array was offset to leave only MXB 1728−34 in the collimator response; this confirmed that the Rapid Burster was active. At 17:46 UT the satellite pointing was changed so that MXB 1728−34 was excluded from the FOV, but with the Rapid Burster at 48% transmission efficiency. This pointing was maintained until the end of the observation. The ME was operated in a coaligned configuration with seven argon-filled detectors, corresponding to a total on-axis effective area of ~1200 cm^2 (see Turner, Smith, and Zimmermann 1981).

For most of the observation the total counting rate from the ME argon detectors (1–15 keV) was sampled with a frequency of 256 Hz (~4 ms accumulation interval). Between 06:45 and 07:52 UT the sampling resolution was increased to 1024 Hz (~1 ms). For about one-half of the observation (between 15:30 and 23:12 UT) 32 channel argon energy spectra were recorded with a time resolution of either 0.312 s or 0.156 s. Over the rest of the time eight energy channel data were recorded every 0.094 s. Energy spectra with 8 s time resolution and 256 channels were also obtained throughout the observation with the ~100 cm^2 gas scintillation proportional counter (GSPC; Peacock *et al.* 1982).

Figure 1 (Plates 17–20, *lower panels*) shows the 1–15 keV intensity profiles with 32 s time resolution given in terms of the observed counts per second (counts s^{-1}) from all the ME argon detectors. Persistent emission from MXB 1728−34 contributes during the first 2.3 hr of the observation; the decrease in count rate at 17:46 UT occurs when the pointing was changed. The period during which half the ME detector array was offset is indicated by arrows (the peak burst count rate was about halved because only four out of seven ME detectors were pointed toward the Rapid Burster). A total of 40 type 2 bursts were observed. In addition, one type 1 burst (between burst 8 and 9) was observed. This most likely came from MXB 1728−34 because the spectrum at burst maximum was very hard, with $kT \approx 3.5$ keV for a blackbody fit (see also Hoffman *et al.* 1979). This is much harder than the 2–2.5 keV typically measured at the peak of type 1 bursts previously observed from the Rapid Burster (Marshall *et al.* 1979; Barr *et al.* 1987). The type 2 bursts varied substantially in their duration (by a factor of ~9), and peak flux (by a factor of ~3). Persistent emission was also observed from the Rapid Burster. Its flux, between bursts, varied typically by a factor of ~2, and occasionally showed brief flares (see, e.g., Fig. 1*a*, and Fig. 2 [Pl. 00], *bottom panel*). The persistent flux briefly dips shortly before and after each burst. A similar effect has been observed during previous observations when "flat-topped" bursts lasting 35–50 s were emitted (Lewin 1977*a*; van Paradijs, Cominsky, and Lewin 1979; see also Lewin *et al.* 1976).

In Table 1 we summarize the burst properties. The burst numbers correspond to those in Figure 1. The typical burst peak fluxes and the burst intervals evolved substantially throughout the observation, on a time scale of hours. The shortest bursts (e.g., bursts 13–16, and 25–27), which lasted 1.5–2 minutes had higher peak luminosities than the longer bursts (see, e.g., burst 29 which lasted ~11 minutes).

III. QUASI-PERIODIC OSCILLATIONS

a) Analysis Technique

The ~4 ms and ~1 ms argon intensity data were analyzed with a fast Fourier transform (FFT) algorithm to investigate the short-term variability of the X-ray flux from the Rapid Burster. While no evidence was found for coherent oscillations (up to a Nyquist frequency of 512 Hz), strong QPO were detected with a centroid frequency varying between 0.4 and 5.0 Hz. To characterize the QPO properties we calculated the power spectra of the 31.25 ms rebinned data for individual 16 s intervals. The upper panels of Figure 1 show power spectra obtained as a function of time in the range from 0.03 to 8 Hz. Each power spectrum (32 s of data) represents the average of two consecutive 16 s power spectra. A gray scale is used to represent the power levels at different frequencies (the more power, the darker the image), such that QPO show up as dark "islands."

b) QPO during Bursts

QPO are detected at frequencies near 4–5 Hz in almost all bursts longer than 3 minutes (these bursts are characterized by relatively low peak flux levels). They are also seen near 2 Hz in eight of the 23 shorter bursts with high peak flux levels. The QPO peak frequency ν_{QPO} during the bursts shows a clear anticorrelation with the average burst intensity I_b, with the brightest bursts showing the lowest frequency (Fig. 3*a*). The power spectra were described quantitatively by fitting a Lorentz profile to the QPO peak and a power law to any possible increase of power toward low frequencies (red noise

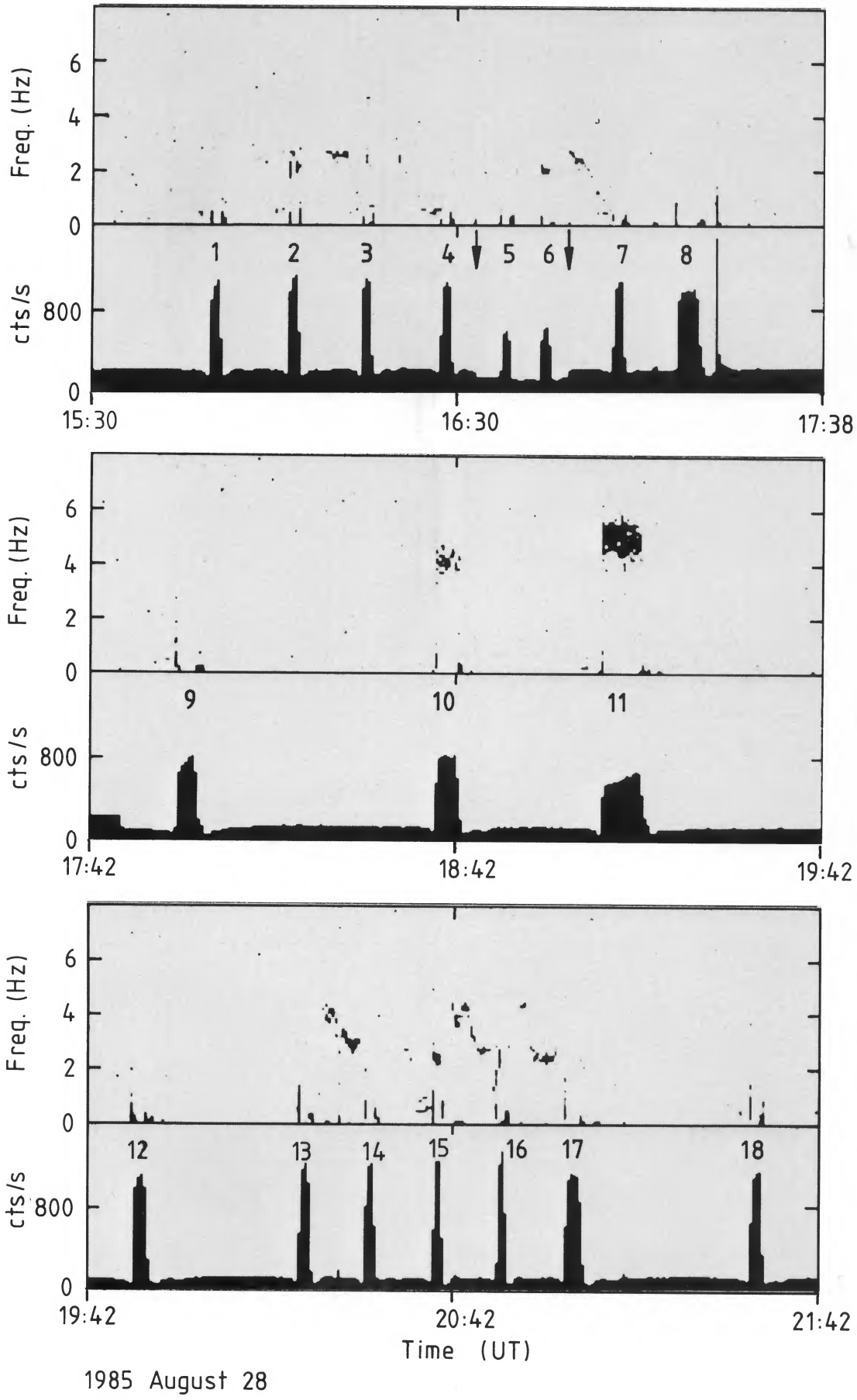

FIG. 1.—1–15 keV count rates (*lower part of each panel*) and power spectra (*upper part of each panel*) vs. time during the 1985 August 28–29 *EXOSAT* observation of the Rapid Burster. Count rates are background subtracted and refer to seven coaligned ME detectors, with the Rapid Burster included at a 48% efficiency in the collimator response. Shade of gray of each point in the upper panels indicates power density measured at the corresponding frequency and time, such that darker shades of gray indicate a higher power. QPO are clearly seen during almost all of the long duration bursts (>2 minutes) and during some of the 1–2 minute long bursts. QPO were also detected in many of the persistent emission intervals between the 1–2 minute long butsts and showed in several instances a characteristic frequency evolution from ~4 Hz to ~2 Hz (see text for further details). Due to the presence of a few short data gaps (not shown) and some nonlinearities in the reproduction process, the accuracy of the time axis is limited to ±1 minute. From 15:30 to 17:46 UT the contribution from the persistent emission of 4U MXB 1728−34 is clearly visible. From 16:33 to 16:50 UT three ME detectors were offset so as to exclude the Rapid Burster from the collimator response. Arrows in the first diagram of (*a*) indicate two minute gaps in the data which are not represented in the time axis. The exponential burst between bursts 8 and 9 was from MXB 1728−34. An excess of power due to background activity is visible near bursts 31, 33, and 40 over a wide range of frequencies.

FIG. 1*a*

PLATE 18

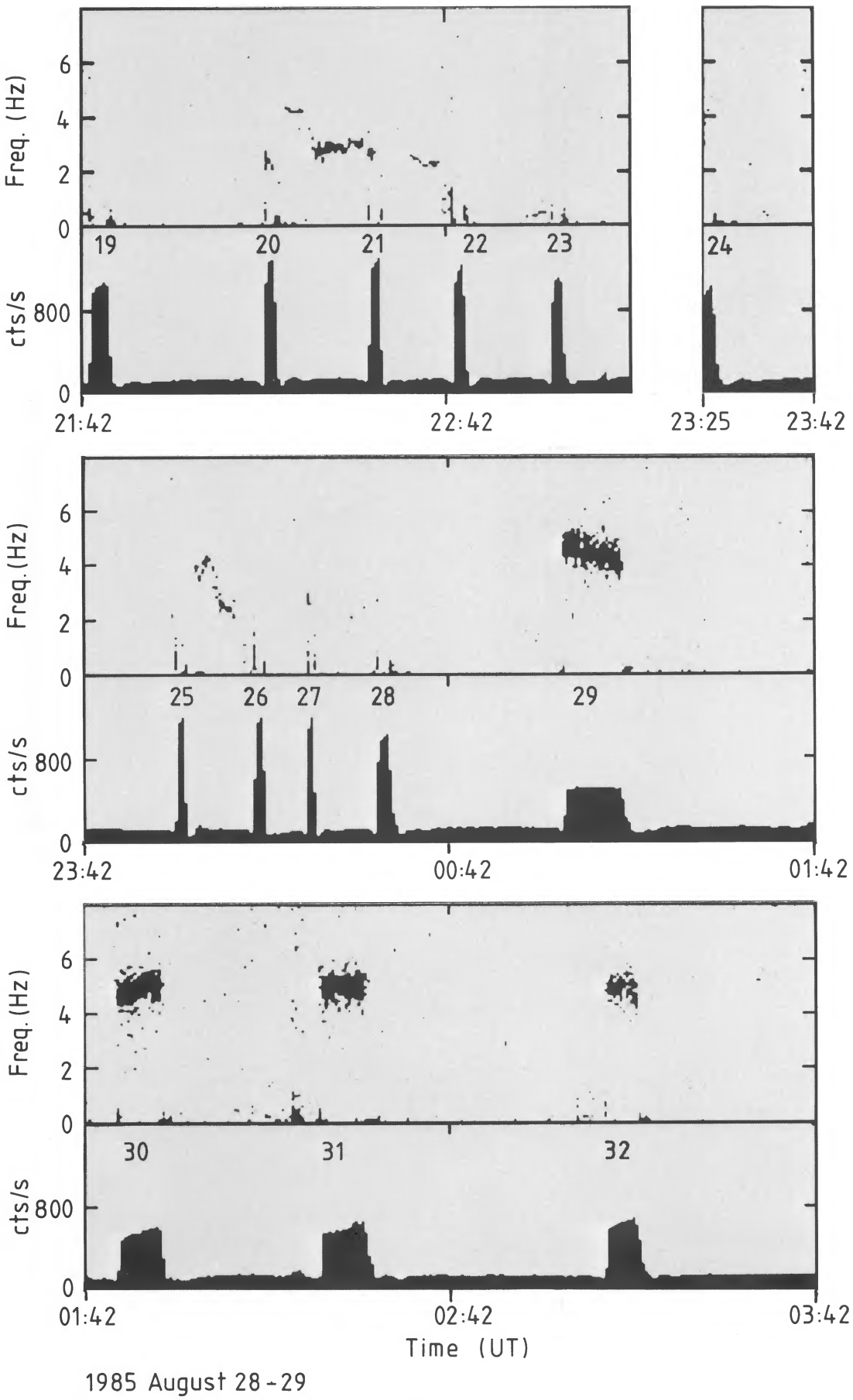

FIG. 1*b*

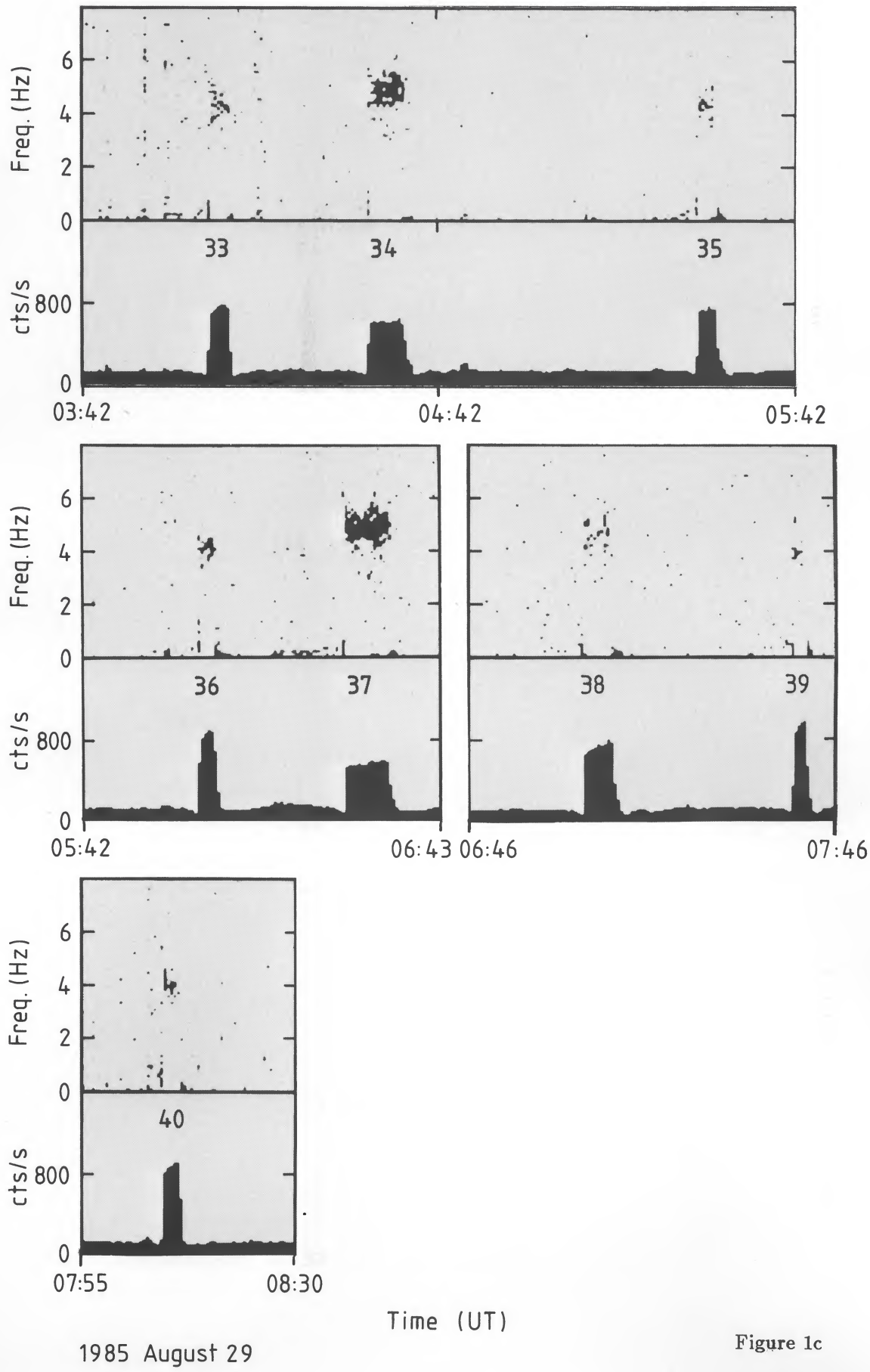

Figure 1c

FIG. 1c

PLATE 20

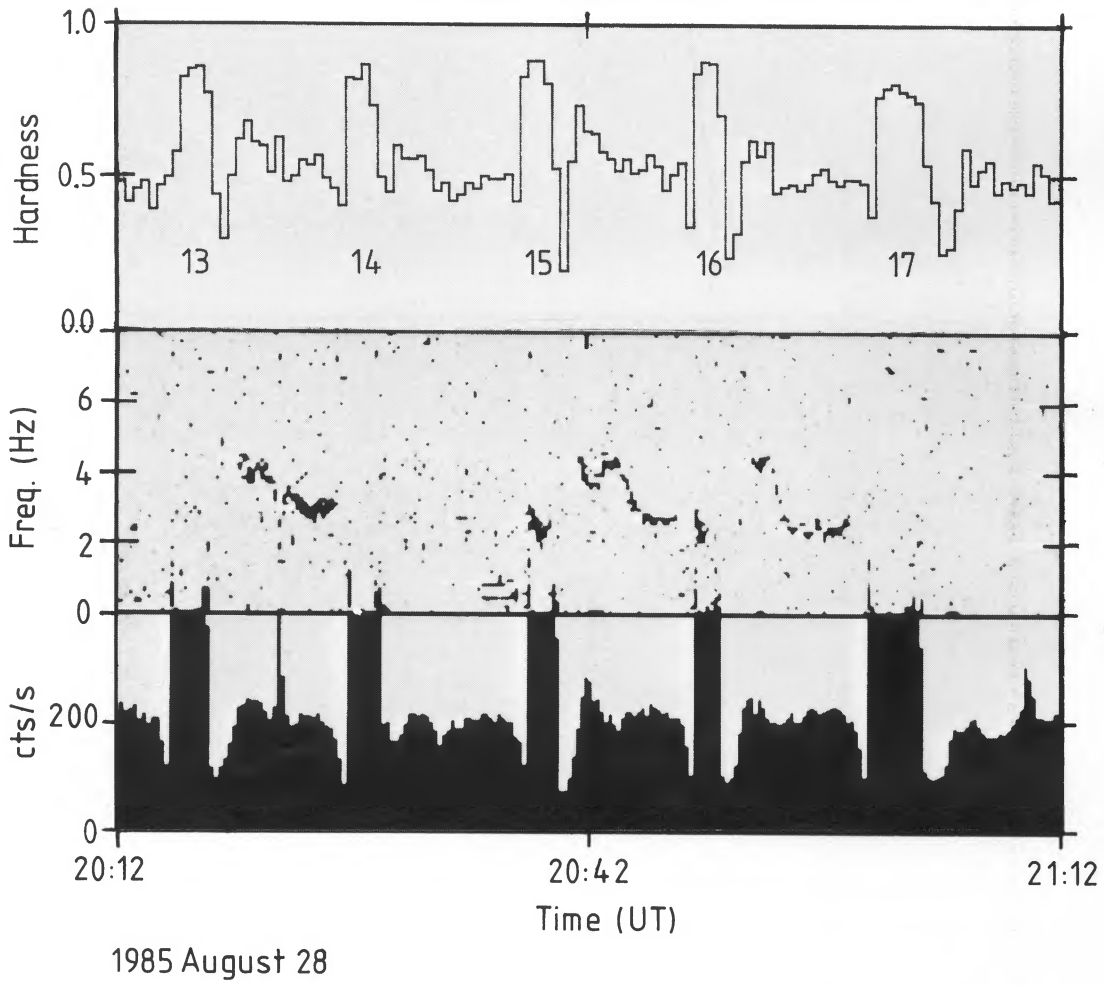

FIG. 2.—1–15 keV count rates (*lower panel*), power spectra (*central panel*), and hardness ratio (5–15 keV/1–5 keV) vs. time for a selected interval in which QPO were observed between bursts. Source intensity and the time axes have been expanded (compared to Fig. 1 [Pl. 00]) in order to make variations in source persistent flux and in QPO frequency more visible. A clear spectral hardening was associated to the bursts. QPO peak frequency between bursts did not show any consistent correlation with source persistent intensity (see also Fig. 5). High-frequency QPO between bursts ($\nu_{QPO} \approx 4$ Hz) corresponded, however, to intervals in which the source spectral hardness was higher (see also Fig. 9).

STELLA *et al.* (*see* **324**, 380)

TABLE 1

Number	UT Day 240+ (1985)	t^+ (s)	F_{peak} (10^{-8} ergs cm^{-2} s^{-1}) (1–20 keV)	E_{burst} (10^{-6} ergs cm^{-2}) (1–20 keV)	F_{per} (10^{-9} ergs cm^{-2} s^{-1}) (1–20 keV)	Width (s) E_b/F_p	QPO peak Frequency (Hz)	QPO FWHM (Hz)	QPO rms Variability (%)	RN rms Variability (0.063–1.0 Hz) (%)
1.....	0.65843	734	2.60	2.78	2.16	107	...	...	<3.3	<2.5
2.....	0.66693	709	2.87	3.08	2.21	109	2.20 ± 0.03	0.14 ± 0.06	6.3 ± 1.3	<2.0
3.....	0.67514	780	2.82	2.80	2.40	99	2.51 ± 0.05	0.15 ± 0.09	3.8 ± 1.0	2.6 ± 0.8
4.....	0.68417	830	2.71	3.04	2.27	112	...	...	<3.0	3.6 ± 0.7
5.....	0.69378	417	2.45	2.35	2.41	96	...	...	<3.1	<6.0
6.....	0.69861	937	2.63	2.95	2.12	112	2.06 ± 0.03	0.05 ± 0.02	8.4 ± 1.9	2.9 ± 1.0
7.....	0.70946	650	2.77	3.06	2.24	110	...	...	<3.0	4.4 ± 0.7
8.....	0.71698	2571	2.42	5.77	2.40	239	...	...	<3.8	2.6 ± 0.6
9.....	0.74674	2474	1.83	3.66	2.35	200	...	...	<3.2	1.7 ± 0.9
10.....	0.77538	1690	1.84	4.46	2.25	242	4.17 ± 0.04	0.38 ± 0.08	7.5 ± 0.8	1.7 ± 0.6
11.....	0.79494	2663	1.31	5.88	2.32	449	4.97 ± 0.03	0.57 ± 0.04	16.8 ± 4.7	1.3 ± 0.8
12.....	0.82576	1550	2.61	6.60	2.30	136	...	...	<2.0	3.3 ± 0.6
13.....	0.84370	631	2.84	3.06	2.84	108	...	...	<1.8	<3.0
14.....	0.85100	680	3.07	3.09	2.03	101	...	...	<2.4	<1.7
15.....	0.85887	650	3.00	2.72	2.52	91	2.48 ± 0.05	0.19 ± 0.06	5.3 ± 1.1	1.9 ± 0.7
16.....	0.86639	685	3.31	3.18	2.19	96	2.19 ± 0.03	0.09 ± 0.09	4.9 ± 2.2	2.9 ± 0.8
17.....	0.87432	1884	2.72	4.80	2.23	177	...	...	<2.6	6.2 ± 0.8
18.....	0.89613	796	2.71	3.34	2.03	123	...	...	<2.1	2.8 ± 0.6
19.....	0.90534	1670	2.43	4.31	2.06	178	...	...	<3.2	3.7 ± 0.5
20.....	0.92471	953	3.27	3.63	2.59	111	2.33 ± 0.04	0.26 ± 0.07	8.5 ± 1.0	2.7 ± 0.5
21.....	0.93560	840	3.30	3.81	2.31	115	2.60 ± 0.05	0.24 ± 0.09	6.0 ± 0.9	4.2 ± 0.6
22.....	0.94532	1012	3.01	3.70	2.33	123	...	...	<2.6	4.3 ± 0.5
23.....	0.95703	1461	2.67	3.53	2.29	132	...	...	<2.8	4.9 ± 0.6
24.....	0.97394	2046	2.38	...	2.35	...	3.8 ± 0.3	1.3 ± 0.3	6.3 ± 1.3	<4.2
25.....	0.99762	728	2.96	2.28	2.29	77	...	...	<2.3	3.5 ± 0.8
26.....	1.00604	500	2.93	2.90	1.62	99	...	...	<2.3	2.4 ± 0.7
27.....	1.01183	675	3.00	2.19	2.27	73	2.55 ± 0.03	0.04 ± 0.08	2.6 ± 1.2	<4.2
28.....	1.01964	1911	2.44	3.71	2.35	152	...	...	<3.5	2.5 ± 0.6
29.....	1.04176	2860	1.09	6.89	2.25	635	4.50 ± 0.03	0.60 ± 0.03	20.6 ± 0.7	1.4 ± 0.7
30.....	1.07486	1895	1.19	4.90	2.51	411	4.91 ± 0.03	0.46 ± 0.04	17.9 ± 1.5	2.8 ± 0.5
31.....	1.09679	2871	1.29	6.17	2.35	480	5.03 ± 0.03	0.36 ± 0.03	18.3 ± 1.2	3.7 ± 0.4
32.....	1.13002	3330	1.37	5.04	2.39	367	4.91 ± 0.03	0.67 ± 0.06	13.0 ± 0.9	<1.6
33.....	1.16856	1555	1.73	3.68	2.43	213	4.13 ± 0.09	0.65 ± 0.15	7.1 ± 0.9	1.7 ± 0.8
34.....	1.18656	3430	1.35	5.54	2.39	410	4.89 ± 0.04	0.68 ± 0.06	13.1 ± 0.7	<3.9
35.....	1.22626	2100	1.67	3.80	2.31	227	4.42 ± 0.04	0.52 ± 0.23	6.7 ± 0.8	2.3 ± 0.6
36.....	1.25057	1566	2.14	3.96	2.59	185	4.00 ± 0.04	0.41 ± 0.14	7.3 ± 0.9	1.8 ± 0.7
37.....	1.26870	2268	1.21	5.78	2.25	477	4.91 ± 0.03	0.55 ± 0.04	20.3 ± 1.0	3.9 ± 0.4
38.....	1.29495	2176	1.65	5.24	2.65	319	4.63 + 0.08	1.0 ± 0.2	8.2 ± 0.9	1.9 ± 0.7
39.....	1.32013	1639	2.26	4.20	2.67	186	3.99 ± 0.03	0.2 ± 0.1	3.9 ± 0.9	<3.6
40.....	1.33910	...	2.07	3.82	...	184	4.01 ± 0.03	0.29 ± 0.06	6.7 ± 0.8	1.7 ± 0.7

[a] Fluxes are derived directly from the fits to the ME argon spectra for bursts 9–22 and for the corresponding persistent emission intervals. Due to the insufficient spectral resolution (bursts 23–40) or the contaminating flux of 4U MXB 1728−34 (bursts 1–8), the fluxes from the other bursts and persistent emission intervals where determined based on the 1–15 keV count rates. Upper limits are 90% confidence.

[RN]; see van der Klis *et al.* 1985). The fits were performed on the average of the 16 s power spectra from each burst.[5] Some results of the fits are given in Table 1 and Figure 2.

The relation between the average burst count rate I_b and the QPO frequency ν_{QPO} can be expressed either in terms of a linear relation $\nu_{QPO} = a + bI_b$, with $a = (7.1 \pm 0.3)$ Hz and $b = (-3.9 \pm 0.3) \times 10^{-3}$ Hz s counts^{-1}, or by a power-law relation $\nu_{QPO} \approx I_b^{\alpha}$, where $\alpha = (-0.75 \pm 0.09)$. The fit was poor (reduced chi square $\chi_r^2 \approx 100$) in both cases, because, for comparable burst intensity levels, the scatter in QPO frequency is far larger (up to ~20%) than the statistical uncertainty. The centroid frequency of the QPO varied by up to 10% within individual bursts (see Fig. 1). In Figure 4 we plot the source intensity versus QPO frequency relationship during three bursts. The QPO centroid frequency was positively correlated with the burst flux during burst 30, negatively correlated during burst 11, and varied by ~10% during burst 29 without any significant change in the burst intensity. Moreover, the QPO frequency changes during individual bursts do not show any systematic correlation with the spectral hardness changes. During burst 21, QPO were only detected during the first minute of the burst.

The power in the QPO was calculated for each burst and expressed in terms of the rms fractional variation (see, e.g., Lamb 1986). This is shown as diamonds in Figure 3*c*. An anti-correlation of the QPO rms fractional variation with the

[5] The variance of the power in each independent frequency bin was evaluated directly from the scatter around the mean values for $N \geq 10$, where N is the number of 16 s power spectra that were averaged, or from P_i^2/N in the other cases (P_i being the power corresponding to the ith frequency, normalized according to the prescription given in Leahy *et al.* 1983). This, in turn, was confirmed by the direct evaluation of the variance in the spectra with $N \geq 10$.

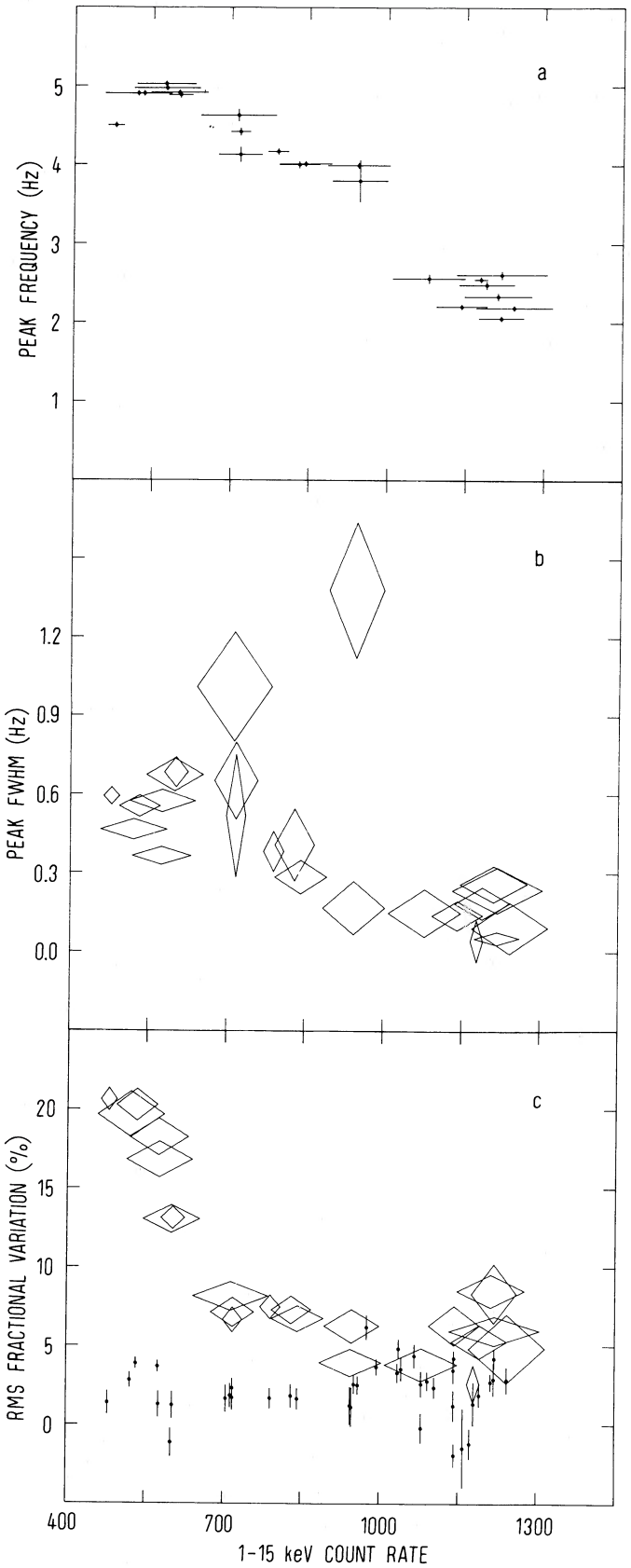

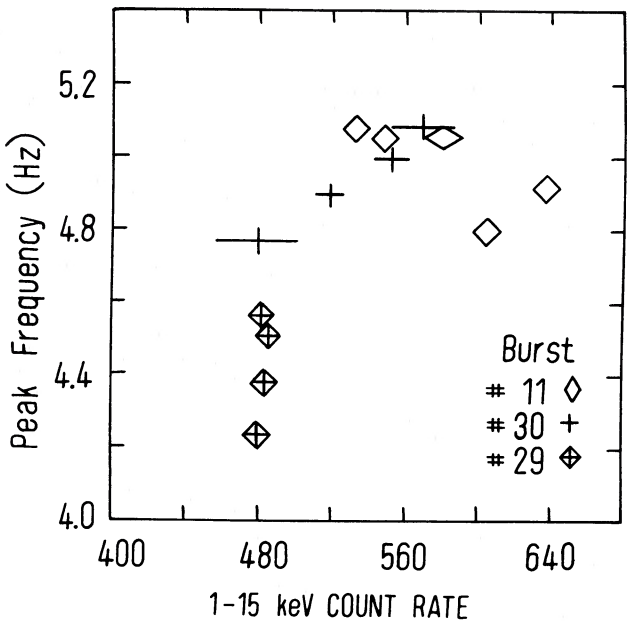

FIG. 4.—QPO peak frequency vs. source count rate during three of the bursts in which frequency changes were observed. The QPO peak frequency can be correlated (burst 30) or anticorrelated (burst 11) with the source intensity within the burst. During burst 29 the QPO frequency varied by ~10% without any significant change in burst intensity.

average burst flux I_b is evident, and the rms fractional variability is as high as ~20% in the low-intensity (and long) bursts. The FWHM of the QPO peaks in the power spectra during bursts varied from 0.04 Hz to 1.3 Hz, with a tendency for the broader peaks to be associated with higher frequency QPO (Fig. 3*b*).

c) QPO in the Persistent Emission

Figure 1 shows that QPO were also present in the persistent emission between some of the relatively short (and most luminous) bursts (e.g., between bursts 13 and 14). In contrast, between the less luminous and long bursts, QPO were never seen, even though the level of the persistent emission was similar. The QPO frequency in most cases decreased from ~4 Hz shortly after a burst to ~2 Hz just prior to the next burst. This evolution of the QPO frequency occurred in several different ways. In some cases the frequency remained approximately constant (e.g., between bursts 2 and 3), while in others a jump from ~4 Hz to ~2.5 Hz occurred in ~1 minute (e.g., between bursts 16 and 17 and between bursts 20 and 21). More complex changes are seen between bursts 15 and 16 and between bursts 25 and 26, where the QPO centroid frequency started near 4 Hz, decreased by ~10% in ~1 minute, then returned to ~4 Hz in roughly the same amount of time before decreasing to ~2.5 Hz (in ~2 minutes). Between bursts 13 and 14 there was an extra complication, a ~1 minute flare occurred during which the QPO frequency decreased by ~25% (see Fig. 2). During this event, the QPO centroid frequency was clearly

FIG. 3.—(*a*) Peak frequency, (*b*) FWHM and (*c*) rms fractional variation (*diamonds*) of the QPO observed during bursts are plotted vs. source count rate. A clear anticorrelation of the peak frequency and of the rms fractional variation with burst intensity is seen. For comparison purposes, the vertical bars in (*c*) represent rms fractional variation of the RN (0.03–1 Hz range) during each of the bursts in which QPO were detected.

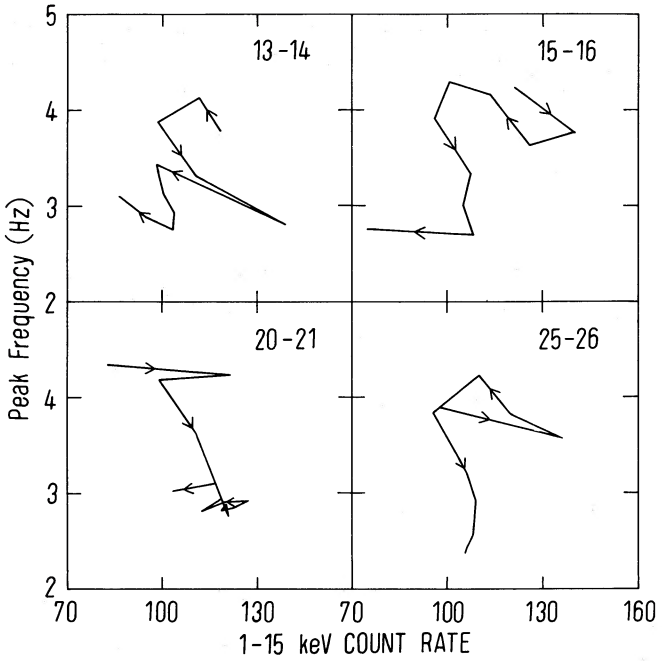

FIG. 5.—Evolution of the QPO frequency in the peak frequency vs. count rate diagram, for the persistent emission intervals between bursts 13 and 14, 15 and 16, 20 and 21, and 25 and 26. No consistent relation is found between the QPO peak frequency and the source intensity between bursts.

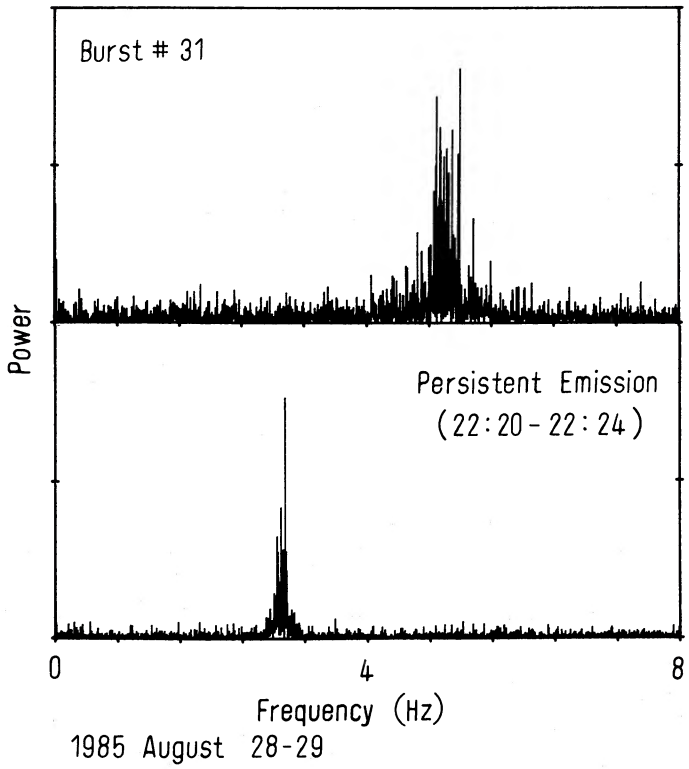

FIG. 6.—High-resolution power spectra (2048 frequency bins) from a 4 minute persistent emission interval bursts 20 and 21 and a 4 minute interval during burst 32. The FWHM of the QPO peak in the persistent emission interval is far smaller than that during bursts.

anticorrelated with the flux in the persistent emission, similar to the relation observed during the bursts. There were other times that a clear correlation was observed (e.g., the remainder of the interval between bursts 13 and 14). However, in general, the correlation coefficient of the QPO frequency with the persistent emission intensity was only 0.098, corresponding to a probability of ~50% of obtaining a higher coefficient from two uncorrelated samples. Therefore, there was no evidence that the QPO frequency was generally either correlated or anticorrelated with the flux of the persistent emission. In Figure 5 we show how the centroid frequency changed with the persistent flux level between a few selected bursts.

The rms fractional variation of the QPO between bursts ranged from the limiting sensitivity (for the count rates observed) of ~8% to values as high as 35%, which are considerably larger than the maximum measured for QPO during bursts. The width of the QPO peak was narrower than that measured during the bursts (even during the bursts in which no clear evolution of ν_{QPO} was observed), with FWHM ranging from 0.03 to 0.3 Hz. This is illustrated in Figure 6, where the high-resolution (2048 frequency bins) power spectrum obtained from a ~4 minute interval between bursts 20 and 21 is shown, together with an analogous spectrum from burst 31.

Significant power-spectrum peaks were also found between 0.4 and 1 Hz during the intervals roughly between 1 and 3 minutes before relatively short bursts (bursts 1, 2, 4, 7, 9, 15, 18, 19, 22, 23, 26; see Fig. 1). These events did not hold a clear connection with the presence of 2–4 Hz QPO in the persistent emission between bursts. The best example of this behavior occurred during the 2 minute interval just before burst 15, where QPO were observed simultaneously at frequencies of (0.44 ± 0.01) Hz and (0.884 ± 0.06) Hz, with FWHM of 0.007 Hz and 0.04 Hz. The rms fractional variation was ~20% and ~15%, respectively (see Fig. 7). The location of the higher frequency peak is consistent with the second harmonic of the peak at ~0.44 Hz.

QPO were not detected in most of the dips which occurred in the persistent emission just before and after the bursts (however, due to the lower count rates the limiting sensitivity to QPO during the dips was ~10% rms). Only in the dips before bursts 4, 15, and 22, QPO with frequencies of 0.5–0.6 Hz and strengths of 13%–22% were found.

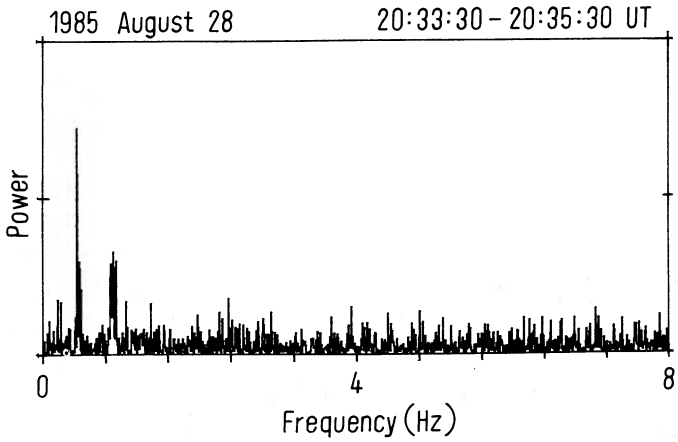

FIG. 7.—High-resolution power spectrum (1024 frequency bins) from the 2 minute interval just before burst 15. QPO are observed at a frequency of ~0.44 Hz. A very significant peak is also observed at a frequency of ~0.88 Hz consistent with the second harmonic of the QPO.

d) Red Noise

All the low-resolution power spectra in which QPO were seen were also used to characterize any power increasing toward low frequencies, i.e., red noise (RN). There was little RN in the power spectra down to frequencies of 0.03 Hz, during both the quiescence intervals, and the "flat-topped" part of the bursts. Only the rise and decay of each burst produced substantial RN with a strength comparable to that of the QPO (see Figs. 1 and 2). In a few power spectra the RN power excess above the counting statistics noise level was only seen in the first one or two frequency bins. Power-law fits to the RN, obtained together with the Lorentzian QPO fits, in most cases did not produce useful results, because the power-law slopes were steeper than -2, where the RN parameters cannot be estimated using Fourier transform techniques (see Deeter 1983). We evaluated the rms fractional variation of the RN by summing the excess power above the level expected from a constant source, in the 0.03–1 Hz range. The rms fractional variation of the RN was determined to be typically 0.2–0.5 times the corresponding QPO rms fractional variation, with values as small as 0.1 during the longer bursts and a few selected quiescence intervals. The results from the power spectra of the bursts are listed in Table 1 and are shown in Figure 3*c* as a function of count rate. Similar conclusions are valid for the persistent emission intervals, where the rms variability of the RN varied between $< 6\%$ and 26% (0.03–1 Hz) and was up to a factor of ~ 6 smaller than the rms variability of the QPO in the persistent emission (when these were detected).

The frequency range was extended toward low frequencies by rebinning the data so that the entire flat topped burst 29 was included in two 4096 point FFTs (but excluding the rise and the decay of the burst; see Fig. 8). The lack of power in the RN persisted, since the RN fractional variation over the 0.0039–1 Hz range was only 1.5%. The QPO rms fractional variation during the same burst was $\sim 21\%$.

e) Background Events

During several periods lasting up to ~ 5 minutes, we observed strong power at all frequencies (i.e., up to 128 Hz) associated with a simultaneous flare in the count rate (see Fig. 1). Since in a few cases the count rate flare was observed in only some of the ME detectors, it can be excluded that these events were due to the Rapid Burster. At least five such background events can be distinguished in Figure 1: one ~ 3 minutes prior to burst 31, two prior to burst 33, one ~ 5 minutes after burst 33, and one ~ 2 minutes before burst 40.

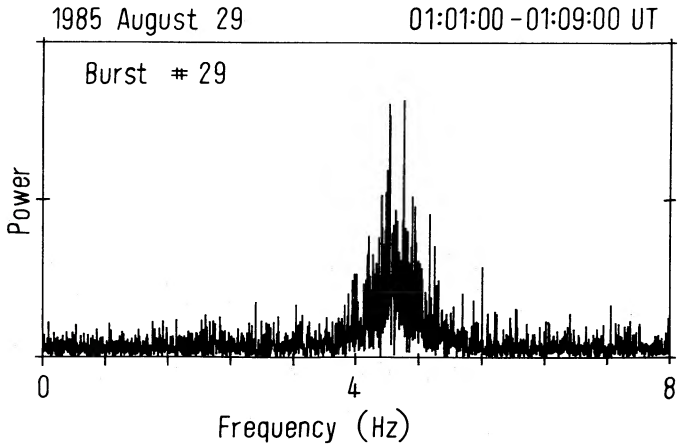

FIG. 8.—High-resolution power spectrum (2048 frequency bins) from an 8 minute interval during burst 29. This comprises the best example of lack of RN.

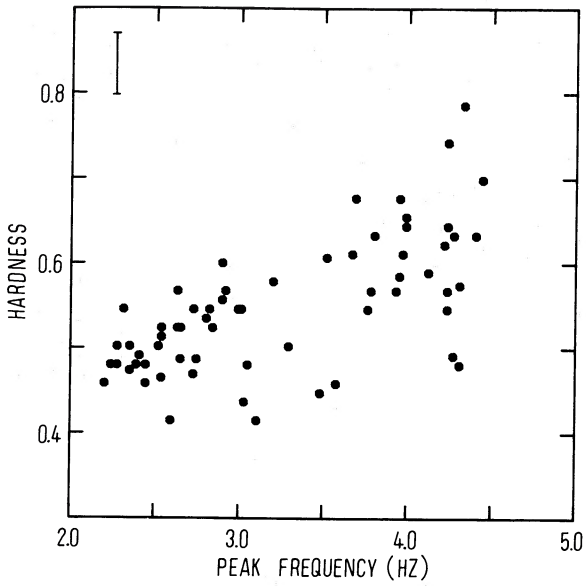

FIG. 9.—Relation between hardness ratio (5–15 keV/1–5 keV) and QPO peak frequency in the persistent emission intervals in which QPO were detected. Characteristic error bar in the hardness ratio axis is plotted in top left corner. The 1 σ uncertainties in the QPO frequency are comparable to the size of the circles plotted. A very significant correlation is found between the QPO frequency and the source spectral hardness between bursts.

IV. SPECTRAL PROPERTIES

A spectral hardness ratio obtained from dividing the counts in the 5–15 keV band by those between 1 and 5 keV (in 16 s intervals) is shown in Figure 2 for a section of the data (*top panel*). The bursts are associated with a spectral hardening when compared to the persistent emission intervals. The sharp decrease in the persistent emission intensity just before and after each burst corresponds to a spectral softening (see Fig. 2), indicating that these decreases are not caused by increased photoelectric absorption. During the persistent emission intervals the spectral hardness seems to be correlated with the QPO frequency (Fig. 2). A linear correlation coefficient of 0.65 was obtained, which for 63 points corresponds to a probability of $\sim 10^{-6}$ of obtaining a larger coefficient from two uncorrelated samples, for the intervals between bursts 13 and 14, 15 and 16, 16 and 17, 20 and 21, 21 and 22, and 25 and 26. The results are shown in Figure 9 (see also Fig. 2).

The 32 and 64 channel ME argon energy spectra of bursts 9 to 22 (obtained by subtracting the off-source particle background) and the corresponding spectra from the persistent emission intervals were analyzed by convolving several trial spectral models through the response function of the ME argon chambers. The simple blackbody spectrum suggested by previous investigations for type 2 bursts from the Rapid Burster (Marshall *et al.* 1979; Barr *et al.* 1987) did not produce acceptable fits to either the burst or the persistent emission spectra, the reduced chi squares obtained being typically $\chi_r^2 \geq 3$. However, an unsaturated Comptonization model, approximated by the function $E^{-\Gamma} \exp(-E/kT_c)$ (see White *et al.* 1986), together with an iron emission line at ~ 6.7 keV, gave

acceptable fits. An average photon power-law index of $\Gamma = -0.66 \pm 0.06$ and -0.89 ± 0.11, a temperature of $kT_c = 2.65 \pm 0.06$ keV and 2.20 ± 0.07 keV, and a column density of $N_H = (1.7 \pm 0.1) \times 10^{22}$ cm^{-2} and $(1.3 \pm 0.1) \times 10^{22}$ cm^{-2} were obtained, respectively, during the 1.5–2 minute long bursts and the very long (>2 minutes) bursts. For the persistent emission spectra instead, average values of $\Gamma = -0.06 \pm 0.21$ and -0.30 ± 0.18, $kT_c = 2.8 \pm 0.3$ keV and 2.4 ± 0.2 keV, and a column density of $N_H = (1.2 \pm 0.2) \times 10^{22}$ cm^{-2} and $(0.9 \pm 0.2) \times 10^{22}$ cm^{-2} were derived during the intervals after the 1.5–2 minute long bursts and after the very long (>2 minutes) bursts, respectively.

The iron emission parameters were evaluated based on the GSPC spectra. A line energy of 6.50 ± 0.07 keV and 6.71 ± 0.05 keV (with a FWHM of 1.4 ± 0.2 keV), and a flux of $\sim 7.3 \times 10^{-3}$ photons cm^{-2} s^{-1} and $\sim 2.2 \times 10^{-3}$ photons cm^{-2} s^{-1} during the bursts and the persistent emission intervals, respectively, were determined. The iron line flux exhibited a less pronounced variability than the continuum between the persistent emission and the bursts, such that the equivalent width ($\sim$200 eV during the bursts) increased by a factor of ~ 2 in the persistent emission.

The spectra from most of the bright low-mass X-ray binaries (LMXRB) display a 1–2 keV blackbody component (in addition to an unsaturated Compton component and an iron line) which contributes from 10% to 70% to the total X-ray flux (see White *et al.* 1986). This was not the case for the Rapid Burster spectra reported here, for which a 5% and 11% upper limit to the contribution of a 1 keV blackbody component was derived, respectively, for the average type 2 burst and persistent emission spectra (these are shown in Fig. 10). The upper limits for a 2 keV blackbody component of 24% and 35%, respectively, are larger because such a spectrum is similar to that of the Comptonized component.

Assuming spherical symmetry and a source distance of 10 kpc (Kleinmann, Kleinmann, and Wright 1976), the average burst peak luminosities varied from a minimum of 1.3×10^{38} ergs s^{-1} (burst 29) to a maximum of $\sim 4 \times 10^{38}$ ergs s^{-1} (e.g., bursts 16 and 21). The time-averaged burst luminosity for the entire observation was 2.6×10^{37} ergs s^{-1} which was $\sim$80% of the time-averaged luminosity between the bursts. Thus the time-averaged luminosity (including both the bursts and the persistent emission) was $\sim 5.8 \times 10^{37}$ ergs s^{-1}. Quoted luminosities are in the 1–20 keV range.

V. DISCUSSION

The Rapid Burster exhibits a complexity in its behavior that to date has no equivalent. The discovery of two different types of bursts from this source in 1977 proved crucial in the understanding of the nature of X-ray bursts in general (Hoffman, Marshall, and Lewin 1978). The thermonuclear ignition of freshly accreted material on the surface of a neutron star provides a convincing explanation for the origin of the type 1 bursts. The cause of the type 2 bursts is not precisely known, but it seems probable that they are the result of an instability in the accretion flow. It is still an open question why these events are unique to the Rapid Burster (some possibly related phenomena in other X-ray sources have been discussed by Lewin and Joss 1983 and, more recently, by Parmar *et al.* 1987). Well-established models for the accretion instability can be divided into two classes. In one class, type 2 bursts are caused by a gating mechanism associated with a neutron star magnetosphere (Lamb *et al.* 1977; Baan 1977, 1979). In the other class of models, the viscous and thermal instabilities of the inner

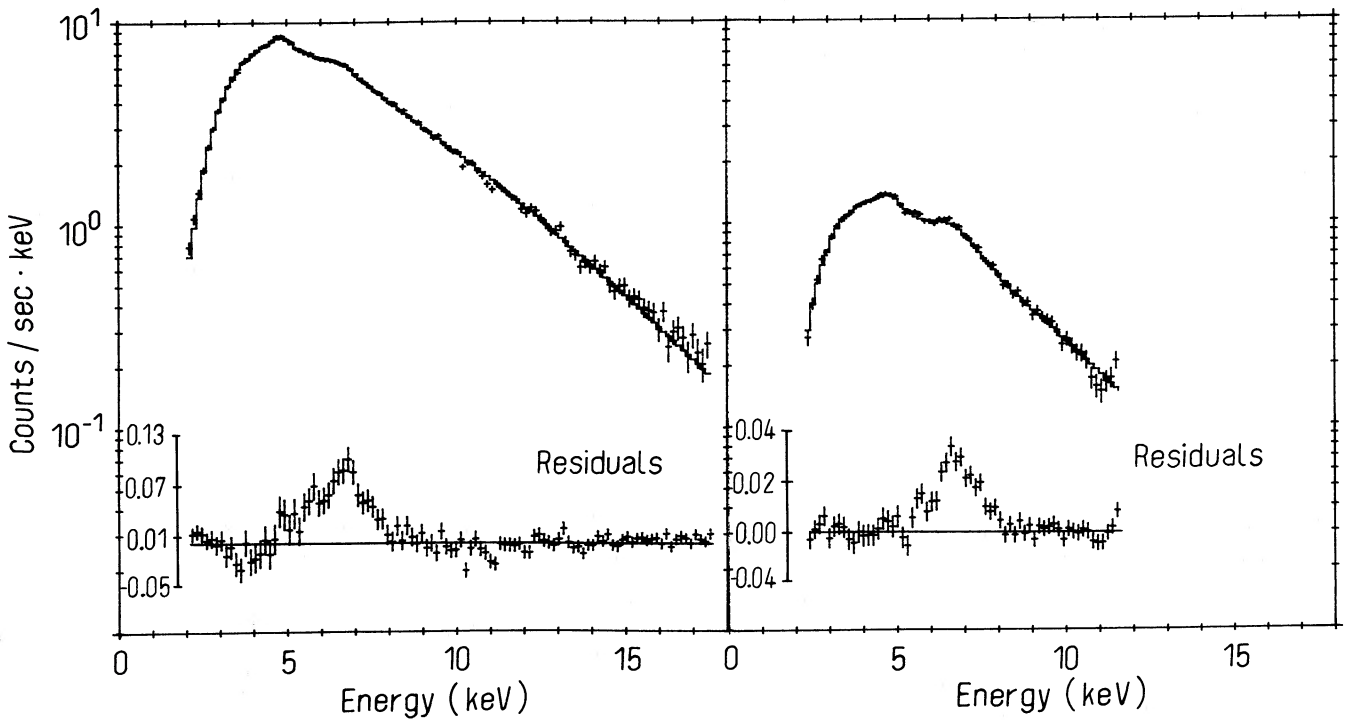

FIG. 10.—Average GSPC energy spectra during the bursts (*left*) and during the persistent emission (*right*). The best-fit models discussed in text are also plotted. Graphs at bottom show the iron line emission profile in the two cases.

radiation pressure dominated region of an accretion disk (which extends close to the neutron star surface) are responsible for the highly spasmodic accretion which gives rise to the type 2 bursts (Taam and Lin 1984; Meyer 1986).[6]

The interpretation of the recently discovered QPO phenomenon in LMXRB likewise revolves around two basic scenarios involving either the interaction of a magnetosphere with the accretion flow, or phenomena occurring in the innermost regions of an accretion disk around a weakly magnetized neutron star. In GX 5−1 (van der Klis *et al.* 1987*a*), Cyg X-2 (Hasinger 1986), Sco X-1 (Priedhorsky *et al.* 1986; van der Klis *et al.* 1987*b*) and GX 17+2 (Stella, Parmar, and White 1987) the occurrence of QPO is restricted to specific spectral or activity states, or both. The complexity of the QPO in the Rapid Burster as reported here is unlike that of other X-ray sources that exhibit QPO (for references see § I). This complexity could again provide a key, this time to our understanding of the origin of QPO and, in turn, of the accretion instability that produces the type 2 bursts. Before considering QPO models in detail we begin with a summary of the QPO properties of the Rapid Burster.

a) QPO in the Type 2 Bursts

QPO were observed in more than half of the 40 type 2 bursts reported here. They were particularly prominent (although not exclusively) during the least luminous, bursts, which were also the longest and the most energetic bursts (see Fig. 1 and Table 1). One distinct feature of the QPO during type 2 bursts is that the centroid frequency averaged over each burst (which ranged between ∼2 Hz and ∼5 Hz) was anticorrelated with the average peak burst flux (Fig. 3*a*). Yet the relation between the instantaneous QPO frequency and the instantaneous burst flux within each burst was not unique (Fig. 4), showing scatter in frequency up to ∼20% ("instantaneous" here refers to the individual 32 s power spectra).

QPO were not detected in 17 type 2 bursts, with upper limits to the rms variation of typically 1.5%–2.5%. Overall the bursts in which QPO were absent tended to be relatively short (<2 minutes), there was nothing unusual to distinguish bursts that did or did not show QPO. For example burst 14 (with no detectable QPO) and burst 15 (with QPO) were very similar with respect to their peak fluxes, total energies, and spectral hardness, as well as the intervals before and after the two bursts (Figs. 1–2, Table 1). In 1979 August, Tawara *et al.* (1982), using *Hakucho*, observed ∼2 Hz QPO in two of 63 type 2 bursts (the 63 bursts lasted between 0.7 and 10 minutes). The two bursts in which QPO were observed lasted each ∼2 minutes. Many of the other 61 bursts had similar flux and duration as the two in which QPO were observed (Tawara *et al.* 1982).

Thus the strength of QPO during a burst is not uniquely determined by the peak flux, total energy, or spectral hardness of the burst. We note, however, that all type 2 bursts that we observed and that lasted more than ∼4 minutes exhibited QPO.

b) QPO in the Persistent Emission

QPO were on some occasions also observed in the persistent emission intervals after the most luminous (i.e., the shortest and least energetic) type 2 bursts; they were not detected during burst intervals longer than $\sim 10^3$ s. The persistent emission and the QPO between the bursts (when observed) seem to follow a pattern. Just before and after the type 2 bursts, dips occurred in the persistent emission (see van Paradijs, Cominsky, and Lewin 1979) which were associated with a spectral softening and, therefore, were not the result of increased absorption (see top panel of Fig. 2). In several intervals after a burst, the QPO became detectable (near ∼4 Hz) when the count rate and the spectral hardness reached a maximum (∼2 minutes after the burst terminated). The general tendency for the QPO frequency was to decrease thereafter from ∼4 to ∼2 Hz. Superposed on this general trend, significant changes occurred on a time scale of minutes. The ∼2 Hz QPO disappeared well before the onset of the next type 2 burst. There was a clear positive correlation between the QPO frequency and the spectral hardness of the persistent flux, although no correlation existed between the QPO frequency and the persistent flux level.

QPO frequencies below 1 Hz were observed only in the persistent emission. In most cases these low QPO frequencies occurred prior to the dips preceding a burst, but in three cases they were detected during the dip itself. Whether or not the <1 Hz QPO occurred before or during the dips was independent of whether 2–4 Hz QPO were seen during the same persistent emission interval.

During the 1985 August 28–29 observation of the Rapid Burster, the time-averaged persistent flux between the type 2 bursts was ∼1.2 times the time-averaged burst flux. Previously reported values for the time-averaged persistent flux in the presence of type 2 bursts ranged between less than 20% to 100% of the time-averaged flux in type 2 bursts (White *et al.* 1978; Kunieda *et al.* 1984*a*, *b*). Thus the Rapid Burster appears to be capable of emitting type 2 bursts in combination with low, as well as high, levels of persistent emission.

c) Strength of the QPO

The strength (rms fractional variation) of the QPO in the bursts (when observed) was roughly anticorrelated with the average burst flux (Fig. 2*c*). It had maximum values near 20% during the least luminous (longest and most energetic) bursts (29, 30, 31, 37). During the persistent emission the strength of the QPO could be as high as ∼35% in the 2–5 Hz QPO and ∼30% in the 0.5–1 Hz QPO. Tawara *et al.* (1982) observed ∼2 Hz QPO with a strength of ∼10% in two type 2 bursts, whereas in the other 61 bursts no QPO were observed, with upper limits to the strength of ∼4% rms.[7]

During the 1983 *EXOSAT* observations (Barr *et al.* 1987), when the Rapid Burster showed only persistent emission and type 1 bursts, no QPO were detected, with upper limits to the strength of ∼10%. Most previous observations of the Rapid Burster with *SAS* 3 and *Hakucho* were carried out at a moderate time resolution (≥0.4 s) which prevented any investigation of the 2–5 Hz QPO.

[6] An alternative scenario involving an accretion instability in the region between the neutron star surface and the radius of the marginally stable orbit ($=6\ GM/c^2$ for a Schwarzschild metric) has been recently suggested by Milgrom (1987). The possible relevance of this instability region in the generation of QPO in LMXRB has also been discussed by Paczyński (1987).

[7] The values given by Tawara *et al.* (1982) in "pulsed fraction" have been rescaled here to rms fractional variability to allow easy comparison with the *EXOSAT* results.

d) Type 2 Bursts and QPO Models

The relaxation oscillator character of the type 2 burst recurrence behavior of the Rapid Burster (Lewin *et al.* 1976) strongly suggests a picture of a reservoir of matter; in this reservoir "pressure" builds up to a critical level at which the reservoir suddenly releases matter that accretes onto the neutron star. In view of the disappearance of the ~ 2 Hz QPO and the appearance (sometimes) of 0.4–1 Hz QPO a few minutes before the onset of the next type 2 burst, the mechanism that causes the QPO apparently "knows about" the state of the reservoir. Thus, either the QPO mechanism originates in or near the reservoir or, if the QPO originate near the surface of the neutron star, there has to be a communication channel between the reservoir and the neutron star surface (e.g., via the accretion flow). Since, just before a burst, we observe in several cases a dramatic change in the QPO characteristics (see above) without any noticeable change in the level or hardness of the persistent emission, it appears to be more likely that the QPO originate in the reservoir rather than very close to the neutron star surface.

This rules against (at least in the case of the Rapid Burster) QPO models involving neutron star oscillations (see van der Klis *et al.* 1985; McDermott and Taam 1987), or magnetic structures emerging from a differentially rotating boundary layer between an accretion disk and the surface of a slowly rotating, weakly magnetized neutron star (Hameury, King, and Lasota 1985). In any case, the magnetic loops responsible for the generation of the "boundary layer spots" in the latter model are probably too short lived to explain the characteristic coherence time [$\sim(\pi\mathrm{FWHM})^{-1} \geq 10$ s] of the 0.44 Hz QPO in the Rapid Burster (J. P. Lasota, private communication in Lewin 1986*a*, *b*).

In the scattering accretion disk corona model for QPO proposed by Boyle, Fabian, and Guilbert (1986), the relation between the source intensity and the QPO frequency is predicted to vary in response to changes in the source X-ray spectrum, since this, in turn, determines the structure of the Compton-heated disk corona. The observed correlation between the source spectral hardness and the frequency of the 2–4 Hz QPO in the persistent emission between is in qualitative agreement with this bursts model. However, a similar correlation is not found for the QPO detected during bursts.

The high values of the QPO strength during the *EXOSAT* observation discussed here and those of Tawara *et al.* (1982) is not in agreement with models where a limited amount of energy is available for the QPO (the scattering corona model of Boyle, Fabian, and Guilbert 1986 and the plasmoid model of Morfill and Trümper 1986; for details see the discussion in Lewin 1986*a*, *b*).

Magnetospheric models in which the QPO frequency represents the Keplerian frequency of the innermost regions of an accretion disk that is disrupted at the magnetospheric boundary (Bath 1973) can also be excluded as the explanation for the 0.44 Hz and, probably, the 2–5 Hz QPO in the Rapid Burster. The former (latter) frequency would lead to a radius of the magnetosphere of $\sim 3 \times 10^8$ cm ($\sim 1 \times 10^8$ cm) and a magnetic dipole field strength of the neutron star of $\sim 10^{12}$ G ($\sim 10^{11}$ G) (for an assumed mass accretion rate of 4×10^{-9} $M_\odot$ yr^{-1}), i.e., similar to that of typical accretion-driven X-ray pulsars. The failure to detect coherent X-ray pulsations would then be unusual. In addition, type 1 bursts have never been observed from an X-ray pulsar.

In the beat frequency model (BFM), the QPO frequency is explained in terms of the difference between the Keplerian frequency ν_m of the accretion disk at the magnetospheric boundary and the rotation frequency ν_0 of the neutron star (Alpar and Shaham 1985; Lamb *et al.* 1985; Berman and Stollman 1986; Lamb 1986; Morfill and Trümper 1986). Under the assumption that the source intensity I_b is proportional to the mass accretion rate $\dot{M}$ the neutron star rotation frequency can be derived, as well as the magnetic dipole field strength (van der Klis *et al.* 1985; but see White and Stella 1987). The latter is lower than that found with magnetospheric models where ν_{QPO} coincides with ν_m (Bath 1973). The absence of coherent pulsations at the neutron star rotation frequency is still a problem, although the low magnetic-field strength ($\sim 10^{10}$ G) and, possibly, electron scattering in a central corona may decrease the pulsation amplitude and prevent their detection (Brainerd and Lamb 1987).

BFMs can be tested only if one has an idea of how the observed X-ray flux is related to $\dot{M}$ (see Lewin 1986*a*, *b*). That this relation may already not be unique has been recently shown by Priedhorsky (1986) in the case of Sco X-1 (Priedhorsky *et al.* 1986; van der Klis *et al.* 1987*b*). One way for the BFM to explain both a positive ($\nu_{\mathrm{QPO}} \approx I_b^\alpha$ with $\alpha > 0$) and a negative ($\alpha < 0$) correlation between QPO frequency and source intensity is to assume that the magnetospheric radius becomes, respectively, smaller and larger than the corotation radius (i.e., the radius at which the Keplerian frequency equals ν_0). While in the former case accretion is possible, in the latter case the centrifugal forces exerted on the material at the magnetospheric boundary is larger than the gravitational force and only little if any accretion takes place.

If we were to accept this interpretation, the anticorrelation between ν_{QPO} and I_b observed during the type 2 bursts from the Rapid Burster would require that they are produced in the intervals in which only little (or no) accretion takes place. This is opposite to the common belief that the "reservoir" of energy for the type 2 bursts is located above the neutron star surface and that the bursts arise from an instability causing part of the matter in the reservoir to be suddenly accreted.

Magnetospheric models have been proposed for type 2 bursts (Baan 1977, 1979; Lamb *et al.* 1977). In the Lamb *et al.* (1977) model the effects due to the rotation of the magnetosphere are not explicitly taken into account; this makes the relation with BFMs for QPO unclear. In Baan's model a reservoir of matter "floats" on top of the neutron star magnetosphere and is partly supported by centrifugal forces. During the intervals between bursts the magnetosphere is assumed to be somewhat larger than the corotation radius. The magnetospheric boundary gradually shrinks in size due to the increased "pressure" of the matter accumulating outside. Type 2 bursts occur when the magnetosphere has become smaller than the critical radius at which the effective gravity (as resulting from gravitational and centrifugal accelerations and the effects of magnetic tension and buoyancy) becomes positive and Rayleigh-Taylor instabilities can develop. This model is consistent with the observed decrease in QPO frequency during the persistent emission if the critical radius is close to the corotation radius, since the modulus of the difference of ν_m and ν_0 (which in the BFM gives ν_{QPO}) decreases as the magnetospheric radius approaches the critical radius before the burst onset. However, the model does not address in detail how persistent emission can be generated between bursts; therefore the relation between the QPO frequency and the persistent emission flux cannot be addressed within this model.

There is no detailed picture about the mechanism which

produces the type 2 bursts in the Baan model, although the observed anticorrelation between ν_{QPO} and I_b implies that the channel in the reservoir (that causes a burst) is smaller, the further the magnetospheric boundary has penetrated inside the corotation radius.

A model in which the type 2 bursts are the result of the viscous and thermal instabilities of the inner radiation-pressure–dominated region of an accretion disk (independent of the possible presence of a magnetosphere) has been proposed by Taam and Lin (1984, see also Meyer 1986). In this scenario at the onset of a burst, while the bulk of the accreting matter flows toward the compact star, an outward-moving wave forms in the innermost disk regions, which propagates toward larger radii and stops at the radius where the radiation pressure equals the gas pressure. If the accretion disk thickens as the wave passes outward, QPO could be generated by an oscillating accretion disk rim which (partially) obscures the central X-ray source (Stella 1986; van der Klis *et al.* 1987*b*). In particular, if the disk can be described by a steady state solution (see Shakura and Sunyaev 1973) and if the source flux is proportional to the mass accretion rate, it is easy to show that the (Keplerian) eigenfrequency of the disk oscillations (see Blumenthal, Taam, and Lin 1984) at the radius at which radiation pressure starts dominating the disk is proportional to $I^{-8/7}$ (Stella 1986). This is in reasonable agreement with the $\nu_{QPO} - I$ relation measured during the type 2 bursts reported here.

The Taam and Lin (1984) model does not, however, address the relaxation oscillation recurrence of the type 2 bursts; neither does the obscuration model described above explain the generation and evolution of the QPO in the persistent emission.

e) Red Noise

Another constraint for the models comes from the RN strength during the bursts, which was usually far lower than the QPO strength. The RN strength varied between $\sim 1.3\%$ and 6%, and was independent of the average burst flux. There was no correlation either between its strength and that in the QPO (Fig. 2*c*). Similar results were found for the RN in the persistent emission. The RN strength (ranging from $<6\%$ to 26%) was usually substantially smaller than that of the QPO (10%–35%) when the latter were present. This near absence of RN in the presence of strong QPO was also observed (although not as extreme) in Sco X-1 (Priedhorsky *et al.* 1986; van der Klis *et al.* 1987*b*). Most QPO sources show instead a RN strength comparable to the QPO strength (e.g., GX $5-1$; van der Klis *et al.* 1985).

These results argue against QPO models involving radiating blobs whose luminosity oscillates quasi-periodically. Since each blob contributes a positive signal (shot) to the total X-ray flux, the presence of QPO will always be accompanied by a substantial amount of RN, whose power will be at least 2 times higher than that of the QPO. This conclusion cannot be escaped in this class of models, unless there exists a correlation between the phases of the pulsations in different shots (for details, see Lamb 1986 and Shibazaki and Lamb 1987). The relative strengths of the RN and the QPO represent therefore a severe challenge for the simple BFM scenario first proposed by Lamb *et al.* (1985), where for modulated (gated) accretion of blobs at the magnetospheric boundary the RN is "a logical consequence of QPO" (see also Lamb 1986). As pointed out by Shibazaki and Lamb (1987), gated accretion of clumps of matter that show a moderate amount of spatial clustering, e.g., due to the fragmentation of a large clump near the magnetopause, can produce QPO whose power substantially exceeds the RN power.

Alternatively, the low strength of the RN compared to that in the QPO could be explained as a result of obscuration by a disk rim which oscillates around the center of the obscured part of the X-ray source (van der Klis *et al.* 1987*b*). This result also argues against the "boundary layer spot" scenario suggested by Hameury, King, and Lasota (1985), where it is likely that each spot gives a positive contribution to the total X-ray flux.

f) Energy Spectra

The spectra of the type 2 bursts reported here are well represented by an "unsaturated Comptonization model" (White *et al.* 1986); a blackbody spectrum is not acceptable. Poorer quality spectra of type 2 bursts obtained previously had been consistent with a blackbody spectrum (e.g., the five energy channel *SAS* 3 spectra; Marshall *et al.* 1979). An unsaturated Comptonization spectral component is also observed from other LMXRB and has been interpreted in terms of emission from an accretion disk (White *et al.* 1986; White, Stella, and Parmar 1988).

VI. SUMMARY OF MODEL CONFRONTATIONS

The above discussion emphasizes that the dichotomy between magnetospheric and nonmagnetospheric models for the generation of the type 2 bursts from the Rapid Burster is also found in the QPO models proposed to date. The variety of bursting modes has not yet been modeled, neither is it clear why the type 2 burst activity is confined to the Rapid Burster. Also QPO models do not adequately account for the properties observed in the Rapid Burster.

Among scenarios involving a magnetized neutron star, the model (proposed in a different context, where the QPO frequency is the Keplerian frequency at the magnetospheric boundary; Bath 1973), can be excluded as the origin of the 0.44 Hz QPO, and (almost certainly) of the 2–5 Hz QPO from the Rapid Burster, since the former would lead to a very large magnetospheric radius and, consequently, high magnetic field strength ($\sim 10^{12}$ G). One would then expect to detect coherent X-ray pulsations and energy spectra similar to those observed in X-ray pulsars. The plasmoid models proposed by Morfill and Trümper (1986) can be excluded for the Rapid Burster because the very high strength of the QPO modulation in both the persistent emission (up to 35%) and in the bursts (up to 21%) involves an energy release in the QPO far larger than the energy available close to the magnetospheric boundary.

The only class of magnetospheric models which appears not to run into immediate problems, as far as the QPO properties of the Rapid Burster are concerned, are some adapted versions of the beat frequency model (BFM; Lamb *et al.* 1985; Lamb 1986; Shibazaki and Lamb 1987). Unfortunately, the predictive power of these models is small. The absence of coherent pulsations is still a problem for the surviving BFMs (see, however, Brainerd and Lamb 1987).

Nonmagnetospheric models for QPO are still poorly developed and, in most cases, only qualitative predictions can be made. In the oscillating accretion disk corona model proposed by Boyle, Fabian, and Guilbert (1986) it is difficult to see how

scattering could modulate a fraction of the X-ray flux as high as 35% rms.

In view of the changes in the QPO several minutes before the onset of a type 2 burst, it appears unlikely that the QPO can be accounted for by a mechanism that operates close to the neutron star surface. (Alternatively, the "reservoir" which powers the type 2 bursts could also be located close to the neutron star surface). This argues against QPO models involving neutron star oscillations (McDermott and Taam 1987) or magnetic activity at the boundary layer between a weakly magnetized, slowly rotating neutron star and an accretion disk (Hameury, King, and Lasota 1985). In addition, the latter model could probably not explain the coherence of the 0.44 Hz QPO in the Rapid Burster, since the lifetime of the magnetic loops in the boundary layer would then have to be ~ 10 s, and this seems unlikely (Lasota, private communication, in Lewin 1986*a*, *b*).

QPO models involving obscuration of the X-ray source by an oscillating accretion disk rim cannot be excluded (Stella 1986; van der Klis *et al.* 1987*b*). These models are only poorly developed to date, and their predictive power is correspondingly low. Since relatively high inclinations are required for this mechanism, the fact that QPO have already been revealed in at least 10 LMXRB could represent a serious problem for obscuration scenarios.

VIII. CONCLUSIONS

A rich variety of QPO modes from the Rapid Burster has been reported. The comparison of these results with current QPO models leads to the conclusion that most QPO mechanisms proposed to date are not operating in the Rapid Burster (this may not mean that they are not at work in other sources). The only proposed models that might be relevant to the Rapid Burster are some beat frequency models (Lamb 1986; Shibazaki and Lamb 1987) and, possibly, models involving obscuration of a central X-ray source by an oscillating accretion disk rim. The viability of these models remains, however, to be demonstrated. Future modeling should address more specifically the interplay of the type 2 burst and QPO activities.

We thank the members of the *EXOSAT Observatory* team for help with the observation and the data analysis, F. K. Lamb for stimulating discussions, and W. Priedhorsky for helpful comments. W. H. G. L. acknowledges a generous award from the Alexander von Humboldt Stiftung, a John Simon Guggenheim fellowship, and support from the U.S. National Aeronautics and Space Administration (Grant NAG8-571). J. v. P. acknowledges a travel grant from the Netherlands Organization for the Advancement of Pure Research (Z.W.O.).

REFERENCES

Alpar, M. A., and Shaham, J. 1985, *Nature*, **316**, 239.
Baan, W. A. 1977, *Ap. J.*, **214**, 245.
———. 1979, *Ap. J.*, **227**, 987.
Barr, P., White N. E., Haberl, F., Stella, L., Pollard, G., Gottwald, M., and Parmar, A. N. 1987, *Astr. Ap.*, **176**, 69.
Basinska, E., Lewin, W. H. G., Cominsky, L., van Paradijs, J., and Marshall, F. J. 1980, *Ap. J.*, **241**, 787.
Bath, G. T. 1973, *Nature Phys. Sci.*, **246**, 84.
Berman, N. M., and Stollman, G. M. 1986. *Astr. Ap.*, **154**, L23.
Blumenthal, G. R., Yang, L. T., and Lin, D. N. C. 1984, *Ap. J.*, **287**, 774.
Boyle, C. B., Fabian, A. C., and Guilbert, P. W. 1986, *Nature*, **319**, 648.
Brainerd, J., and Lamb, F. K. 1987, *Ap. J. (Letters)*, **313**, 231.
Cooke, B., Stella, L., and Ponman, T. 1985, *IAU Circ.*, No. 4116.
Deeter, J. E. 1984, *Ap. J.*, **281**, 482.
Elsner, R. F., Weisskopf, M. C., Darbro, W., Ramsey, B. D., Williams, A. C., Sutherland, P. G., and Grindlay, J. E. 1986, *Ap. J.*, **308**, 655.
Grindlay, J. E., and Gursky, H. 1977, *Ap. J. (Letters)*, **218**, L117.
Hameury, J. M., King, A. R., and Lasota, J. P. 1985, *Nature*, **317**, 597.
Hasinger, G. 1986, in *IAU Symposium 125, The Origin and Evolution of Neutron Stars*, ed. D. J. Helfand and J. H. Huang (Dordrecht: Reidel), p. 333.
Hasinger, G., Langmeier, A., Sztajno, M., Trümper, J., Lewin, W. H. G., and White, N. E. 1986, *Nature*, **319**, 469.
Hoffman, J. A., Marshall, H. L., and Lewin, W. H. G. 1978, *Nature*, **271**, 630.
Hoffman, J. A., *et al.* 1979, *Ap. J. (Letters)*, **233**, L51.
Inoue, H., *et al.* 1980, *Nature*, **283**, 358.
Joss, P. C. 1978, *Ap. J. (Letters)*, **225**, L123.
Kleinmann, D. E., Kleinmann, S. G., and Wright, E. L. 1976, *Ap. J. (Letters)*, **210**, L83.
Kunieda, H., *et al.* 1984*a*, *Publ. Astr. Soc. Japan*, **36**, 215.
———. 1984*b*, *Publ. Astr. Soc. Japan*, **36**, 807.
Lamb, F. K. 1986, in *The Evolution of Galactic X-ray Binaries*, ed. J. Trümper, W. H. G. Lewin, and W. Brinkmann (Dordrecht: Reidel), p. 151.
Lamb, F. K., Fabian, A. C., Pringle, J. E., and Lamb, D. Q. 1977, *Ap. J.*, **217**, 197.
Lamb, F. K., Shibazaki, N., Alpar, M. A., and Shaham, J. 1985, *Nature*, **317**, 681.
Langmeier, A., Hasinger, G., Sztajno, M., Trümper, J., and Pietsch, W. 1985, *IAU Circ.*, No. 4147.
Leahy, D. A., Darbro, W., Elsner, R. F., Weisskopf, M. C., Sutherland, P. C., Kahn, S. M., and Grindlay, J. E. 1983, *Ap. J.*, **266**, 160.
Lewin, W. H. G. 1977*a*, *Ann. NY Acad. Sci.*, **302**, 210.
———. 1977*b*, *American Scientist*, **65**, No. 5, 605.
———. 1986*a*, in *IAU Symposium 125, The Origin and Evolution of Neutron Stars*, ed. D. J. Helfand and J. H. Huang (Dordrecht: Reidel), p. 333.
———. 1986*b*, in *The Physics of Accretion onto Compact Objects*, ed. K. O. Mason, M. G. Watson, and N. E. White (Berlin: Springer Verlag), p. 177.
Lewin, W. H. G., *et al.* 1976, *Ap. J.*, **207**, L95.
———. 1987, *M.N.R.A.S.*, **226**, 383.
Lewin, W. H. G., and Joss, P. 1983, in *Accretion Driven Stellar X-ray Sources*, ed. W. H. G. Lewin and E. P. J. van den Heuvel (Cambridge: Cambridge University Press), p. 43.
Lewin, W. H. G., van Paradijs, J., van der Klis, M., Jansen, F., Basinska, E. M., Langmeier, A., Sztajno, M., and Trümper, J. 1986, *M.N.R.A.S.*, submitted.
Maraschi, L., and Cavaliere, A. 1977, In *Highlights Astr.*, **4**, 127.
Marshall, H. L., Ulmer, M., Hoffman, J. A., Doty, J., and Lewin, W. H. G. 1979, *Ap. J.*, **227**, 555.
Mason, K. O., Bell-Burnell, S. J., and White, N. E. 1976, *Nature*, **262**, 474.
McDermott, P. N., and Taam, R. E. 1987, *Ap. J.*, **318**, 278.
Meyer, F. 1986, in *Proc. IAU Colloquium 89, Radiation Hydrodynamics in Stars and Compact Objects*, ed. D. Mihalas and K.-H. A. Winkler (Berlin: Springer-Verlag).
Middleditch, J., and Priedhorsky, W. 1986, *Ap. J.*, **306**, 230.
Milgrom, M. 1987, *Astr. Ap. (Letters)*, **172**, L1.
Morfill, G. E., and Trümper, J. 1986, in *The Evolution of Galactic X-Ray Binaries*, ed. J. Trümper, W. H. G. Lewin and W. Brinkmann (Dordrecht: Reidel), p. 173.
Norris, J. P., and Wood, K. S. 1985, *IAU Circ.*, No. 4087.
Paczyński, B. 1987, *Nature*, **327**, 303.
Parmar, A. N., White, N. E., Stella, L., Izzo, C., and Ferri, P. 1987, *Ap. J.*, submitted.
Peacock, A., Anderson, R. D., Manzo, G., Taylor, B. G., Villa, G., Re, S., Ives, J. C., and Kellog, S. 1982, *Proc. 15th ESLAB Symposium*, ed. R. D. Andresen (Dordrecht: Reidel), p. 525.
Priedhorsky, W. 1986, *Ap. J. (Letters)*, **306**, L97.
Priedhorsky, W., Hasinger, G., Lewin, W. H. G., Middleditch, J., Parmar, A. N., Stella, L., and White, N. E. 1986, *Ap. J. (Letters)*, **306**, L91.
Shakura, N. I., and Sunyaev, R. A. 1973, *Astr. Ap.*, **24**, 337.
Shibazaki, N., and Lamb, F. K. 1987, *Ap. J.*, **318**, 767.
Steila, L. 1986, *Proc. Conf. Plasma Penetration into Magnetospheres*, (Colymbari, Greece; Sept./Oct. 1985), ed. N. Kylafis, J. Papamastorakis and J. Ventura (Iraklion: Crete University Press), p. 199.
Stella, L., Parmar, A. N., and White, N. E. 1985, *IAU Circ.*, No. 4102.
———. 1987, *Ap. J.*, **321**, 418.
Stella, L., Parmar, A. N. and White, N. E., Lewin, W. H. G., and van Paradijs, J. 1985, *IAU Circ.*, No. 4110.
Stella, L., White, N. E., and Priedhorsky, W. 1985, *IAU Circ.*, No. 4117.
———. 1987, *Ap. J. (Letters)*, **315**, L49.
Taam, R. E., and Lin, D. N. C. 1984, *Ap. J.*, **287**, 761.
Tawara, Y., Hayakawa, S., Kunieda, H., Makino, F., and Nagase, F. 1982, *Nature*, **299**, 38.
Tennant, A. 1987, *M.N.R.A.S.*, **226**, 971.
Turner, M. J. L., Smith, A., and Zimmermann, H. U. 1981, *Space Sci. Rev.*, **30**, 513.
Ulmer, M. P., Lewin, W. H. G., Hoffman, J. A., Doty, J., and Marshall, H. 1977, *Ap. J. (Letters)*, **214**, L11.
van der Klis, M., Jansen, F., van Paradijs, J., Lewin, W. H. G., van den Heuvel, E. P. J., Trümper, J., and Sztajno, M. 1985, *Nature*, **316**, 225.
van der Klis, M., Jansen, F., van Paradijs, J. Lewin, W. H. G., Sztajno, M., Trümper, J. 1987*a*, *Ap. J. (Letters)*, **313**, L19.
van der Klis, M., Stella, L., White, N. E., Jansen, F. and Parmar, A. N. 1987*b*, *Ap. J.*, **316**, 411.
van Paradijs, J., Cominsky, L. and Lewin, W. H. G. 1979, *M.N.R.A.S.*, **189**, 387.

van Paradijs, J., Lewin, W. H. G., Hasinger, G., van der Klis, M., Penninx, W., Sztajno, M., Langmeier, A. and Jansen, F. 1987, *IAU Circ.*, No. 4308.
White, N. E., Mason, K. O., Carpenter, G. F., and Skinner, G. K. 1978, *M.N.R.A.S.*, **184**, 1P.
White, N. E., Peacock, A., Hasinger, G., Mason, K. O., Manzo, G., Taylor, B. G., and Branduardi-Raymont, G. 1986, *M.N.R.A.S.*, **218**, 129.
White, N. E., and Stella, L. 1987, *M.N.R.A.S.*, in press.
White, N. E., Stella, L., and Parmar, A. N. 1988, *Ap. J.*, in press.
Woosley, S. E., and Taam, R. E. 1976, *Nature*, **263**, 101.

F. HABERL, A. N. PARMAR, L. STELLA, and N. E. WHITE: *EXOSAT Observatory*, Space Science Department, European Space Agency, ESTEC, Postbus 299, 2200 AG Noordwijk, The Netherlands

W. H. G. LEWIN: Massachusetts Institute of Technology, Center for Space Research and Physics Department, Cambridge, MA 02139.

J. VAN PARADIJS: Astronomical Institute "Anton Pannekoek," University of Amsterdam, Roetersstraat 15, 1018 WB Amsterdam, The Netherlands